Adv. Radio Sci., 10, 69–73, 2012
www.adv-radio-sci.net/10/69/2012/
doi:10.5194/ars-10-69-2012

Advances in Radio Science

Scattering centers modeling of non-anechoic measurement environments

K. A. Yinusa, C. H. Schmidt, and T. F. Eibert

Lehrstuhl für Hochfrequenztechnik, Technische Universität München, Arcisstr. 21, 80333 Munich, Germany

Correspondence to: K. A. Yinusa (k.y@tum.de)

Abstract. Near-field measurements are established techniques to obtain the far-field radiation pattern of an Antenna Under Test via near-field measurements and subsequent near-field far-field transformation. For measurements acquired in echoic environments, additional post-processing is required to eliminate the effects of multipath signals in the resulting far-field pattern. One of such methods models the measurement environment as a multiple source scenario whereby the collected near-field data is attributed to the AUT and some scattering centers in the vicinity of the AUT. In this way, the contributions of the AUT at the probe can be separated from those of the disturbers during the near-field far-field transformation if the disturber locations are known. In this paper, we present ways of modeling the scattering centers on equivalent surfaces such that echo suppression is possible with only partial or no information about the geometry of the scatterers.

1 Introduction

In order to determine the far-field radiation pattern of an Antenna Under Test (AUT), measurement of the field distribution can be carried out directly in the far-field. The far-field is the region surrounding the AUT from a radial distance of approximately $2D^2/\lambda$, where D is the largest dimension of the aperture and λ is the wavelength. For electrically small antennas i.e. antennas with small physical size relative to the wavelength, the far-field criteria is met at relatively small distance from the AUT and a controlled environment can be easily provided for direct far-field measurement. A controlled environment is one that averts threats due to weather, security, electromagnetic interference, multipath propagation, etc. Such an environment is often achieved in an anechoic chamber, which is a room shielded to prevent electromagnetic waves penetrating from outside and interior lined with radiation absorbent material (RAM) to prevent reflections off the ceiling and floor of the room. In this way, a free space environment is provided for the AUT and the probe antenna so that only the mutual interactions between the AUT and the probe antenna have influence on the measurement. But for electrically large antennas, the far-field characteristics are satisfied at a relatively large distance from the AUT and indoor measurement will require an anechoic chamber of equally large size. An alternative is to measure the antenna in the radiating near-field; a region extending from a distance of about a wavelength from the aperture to the far-field region (Yaghjian, 1986). Measurement in the near-field reduces the required dimension of the anechoic chamber and the amount of absorbers needed to cover the walls. A near-field far-field transformation (NFFFT) algorithm is then applied on the measured near-field data to obtain the far-field pattern. As the dimension of the AUT becomes larger relative to the wavelength, providing an anechoic chamber becomes expensive even for near-field measurements and it is desirable to have techniques that allow for semi-anechoic or outdoor measurements in exchange for some echo suppression post-processing. Techniques based on the matrix pencil (Sarkar and Pereira, 1995) and fast Fourier transform (FFT) techniques attempt to identify the line-of-sight (LOS) components from a broadband measurement (Loredo et al., 2004). The requirement for a broadband measurement however means that these techniques are not applicable for narrowband antennas and require a substantial increase in the measurement time for broadband antennas. Modal filtering techniques, applicable to measurement on canonical geometries i.e. planar, cylindrical, and spherical scan geometries, such as MARS (Gregson et al., 2009) and IsoFilter™ (Hess, 2011) modify the measurement setup such that higher order modes corresponding to the multipath contributions are excited and identifiable. In source reconstruction techniques (González and Álvarez López, 2011; Cano et al., 2010; Araque Quijano et al., 2011), equivalent current sources over fictitious surfaces enclosing the echo sources are computed alongside those representing the AUT

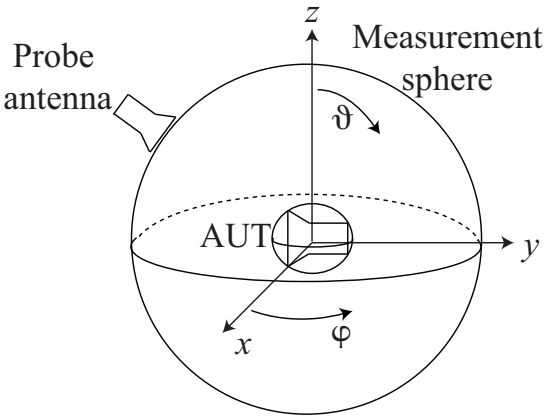

Fig. 1. Measurement setup.

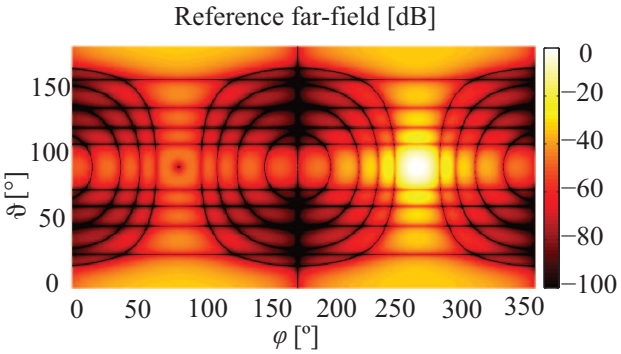

Fig. 2. Reference far-field of the AUT.

such that the AUT far-field can be computed with the isolated AUT equivalent current sources. In the scattering center representation (Schmidt and Eibert, 2009), the echo sources are treated as independent sources contributing to the measured near-field data and with the knowledge of the echo locations, these sources can be integrated into the NFFF transformation algorithm and their contributions can be separated from that of the AUT. The need for echo locations however can be impractical for situations involving several disturbers. In this paper, we present ways of modeling the contributing echo sources such that knowledge of their locations is not necessary for echo suppression. The scattering center representation as implemented in this paper is integrated with a plane wave based near-field far-field transformation algorithm described in Schmidt et al. (2008). A brief description of this algorithm is given in Sect. 2.1 for self-containment. In Sects. 3, 4, and 5, we present scattering centers modeling and results for localized, partially localized, and non-localized echo scenarios, respectively.

2 Preliminaries

2.1 Plane wave based near-field far-field transformation

We consider a spherical near-field measurement setup as illustrated in Fig. 1, where a set of plane waves in all directions $(\bar{\mathbf{I}}-\hat{k}\hat{k})\cdot\tilde{\boldsymbol{J}}(\hat{k})$ with respect to the origin of the coordinate system is used to describe the radiation behavior of the AUT (Schmidt et al., 2008). The recorded probe signal

$$\boldsymbol{U}(\boldsymbol{r}_{\mathrm{M}}) = -j\frac{\omega\mu}{4\pi}\sum_{\hat{k}} T_L(\hat{k},\boldsymbol{r}_{\mathrm{M}})\bar{\mathbf{P}}(\hat{k},\hat{r}_{\mathrm{M}})\cdot(\bar{\mathbf{I}}-\hat{k}\hat{k})\cdot\tilde{\boldsymbol{J}}(\hat{k}) \quad (1)$$

at a measurement point $\boldsymbol{r}_{\mathrm{M}}$ is reconstructed by translating all the plane waves from the AUT to the point $\boldsymbol{r}_{\mathrm{M}}$. $\bar{\mathbf{P}}(\hat{k},\hat{r}_{\mathrm{M}})$ is the probe correction coefficient used to weight the plane waves to compensate for the probe influence and

$$T_L(\hat{k},\boldsymbol{r}_{\mathrm{M}}) = -\frac{jk}{4\pi}\sum_{l=0}^{L}(-j)^l(2l+1)h_l^{(2)}(kr_{\mathrm{M}})P_l(\hat{k}\cdot\hat{r}_{\mathrm{M}}) \quad (2)$$

is the diagonalized translation operator derived from the fast multipole method (FMM) (Coifman et al., 1993) and it converts radiated plane waves from the AUT into incident plane waves at the probe. $h_l^{(2)}$ and P_l are the spherical Hankel function of the second kind and a Legendre polynomial, respectively and k is the wavenumber. The plane wave translation is done in this way to all the measurement points and a linear system of equations

$$\boldsymbol{U} = -j\frac{\omega\mu}{4\pi}\|\mathbf{C}\|\cdot\tilde{\boldsymbol{J}} \quad (3)$$

is formulated with the number of equations and unknowns equaling the number of measurement points and number of plane waves for each polarization, respectively. The system of equations is solved with an iterative solver such as GMRES (Saad and Schultz, 1986) to retrieve the AUT plane wave coefficients.

2.2 Measurement setup

The AUT in the following sections is a 5 GHz square horn antenna with an aperture size of 0.4245 m and a symmetric amplitude and phase excitation. The AUT and echo sources are simulated using dipole distributions and the echoic data is generated by evaluating and superimposing the dyadic Green's function of free space for the individual dipoles at the measurement points. Data is generated for the spherical measurement geometry with a spacing of 3° along ϑ and φ directions at a distance of 0.9 m with the AUT located at the origin of the coordinate system and oriented as shown in Fig. 1. The echo sources are point sources distributed randomly outside the measurement sphere. The reference far-field and far-field with echoes are shown in Figs. 2, and 3, respectively.

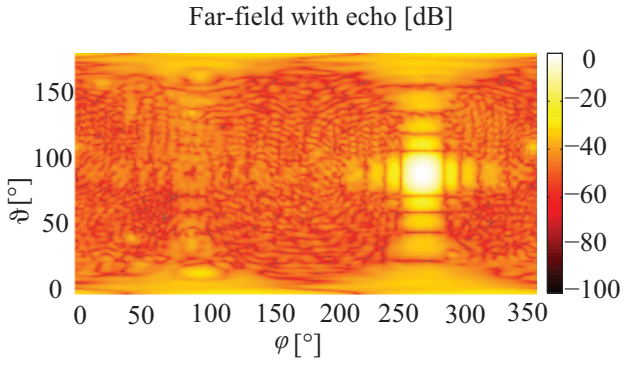

Fig. 3. Far-field with echo: obtained far-field for echoic near-field data without a subsequent echo suppression.

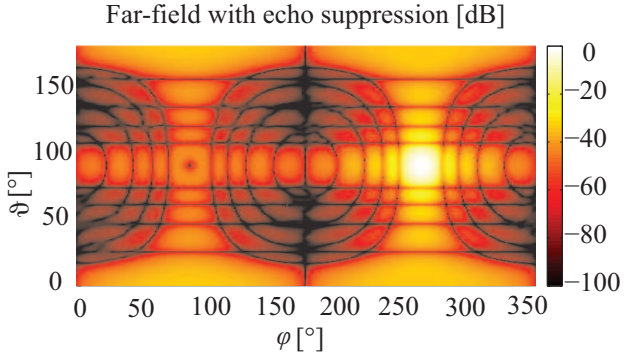

Fig. 4. Far-field after echo suppression with localized echo sources: echo sources are replaced with auxiliary sources at the same locations during the NFFFT.

3 Scattering centers modeling of localized echo sources

The recorded near-field data is a superposition of the field emanating directly from the AUT and multipath signals. The linear system of equations in Eq. (3) can then be rewritten with increased number of unknowns as follows:

$$\boldsymbol{U}' = -j\frac{\omega\mu}{4\pi}\|\mathbf{C}_{\mathrm{AUT}}\|\cdot\tilde{\boldsymbol{J}} - j\frac{\omega\mu}{4\pi}\sum_{i=1}^{N_{\mathrm{SC}}}\|\mathbf{C}_{\mathrm{SC}i}\|\cdot\tilde{\boldsymbol{J}}_{\mathrm{SC}i} \qquad (4)$$

where $\mathbf{C}_{\mathrm{AUT}}$ and $\mathbf{C}_{\mathrm{SC}i}$ represent the coupling matrices for the AUT and the i-th scattering center, respectively. N_{SC} is the number of scattering centers employed. When the echo locations are known, $\mathbf{C}_{\mathrm{SC}}$ can be computed and Eq. (4) is solved to retrieve the plane wave coefficients $\tilde{\boldsymbol{J}}$ of the AUT and $\tilde{\boldsymbol{J}}_{\mathrm{SC}i}$ of the i-th scattering center. Figure 4 shows the far-field pattern after echo suppression.

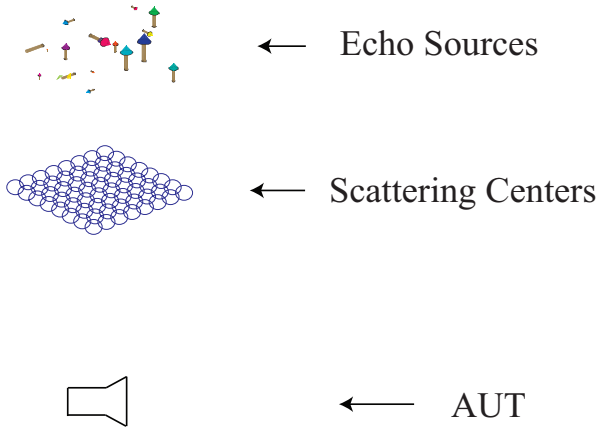

Fig. 5. SCs placed to block the LOS between the AUT and the echo sources.

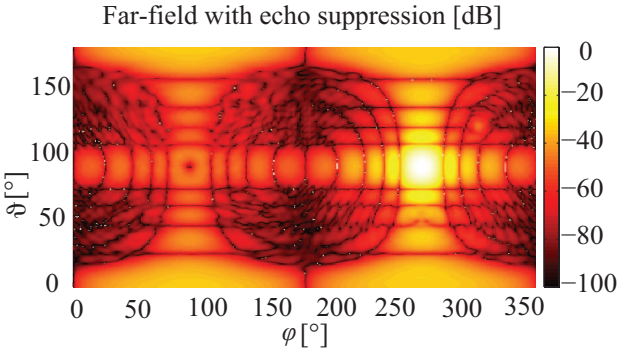

Fig. 6. Far-field after echo suppression with partial knowledge of echo locations.

4 Scattering centers modeling of partially localized echo sources

Often, precise information regarding echo sources is not available and when it is, manual input of large numbers of locations makes it more efficient to combine neighboring echo sources. In these cases, we place the scattering centers along the line-of-sight (LOS) between the AUT and the echo sources such that the measurement geometry is shielded from the target disturbers as shown in Fig. 5. This requires only the knowledge of the direction from which we expect to receive the multipath signals. The result with this representation is shown in Fig. 6 and the difference between the reference and the obtained far-fields before and after echo suppression for $\vartheta = 90°$ cut is plotted in Fig. 7.

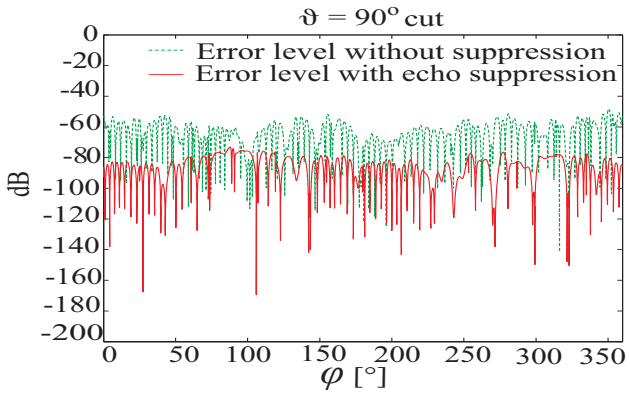

Fig. 7. Error level before and after echo suppression for the representation in Fig. 5.

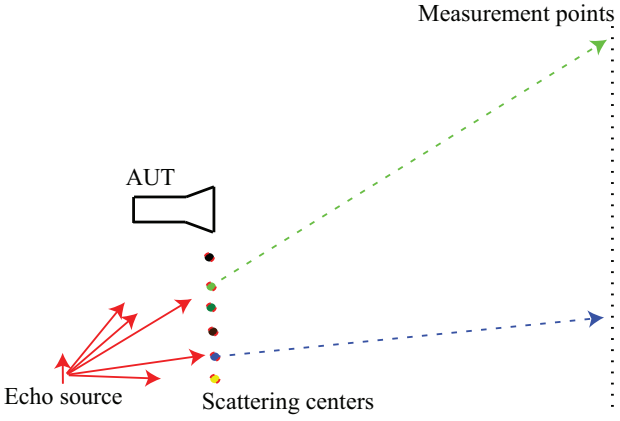

Fig. 8. Several scattering centers can account for contributions of an echo source at different measurement points.

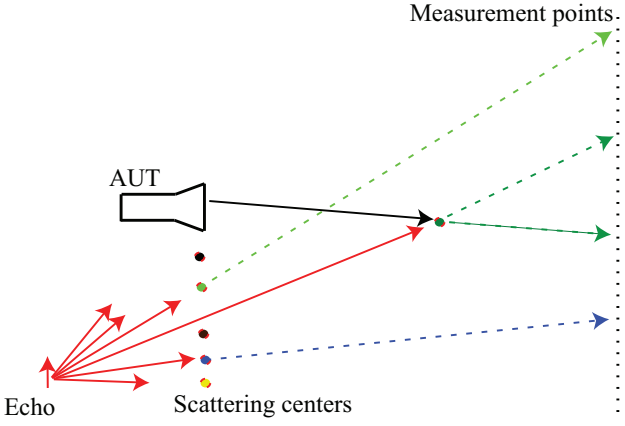

Fig. 9. Scattering centers can also contribute errors in the far-field by replacing components of the AUT signal.

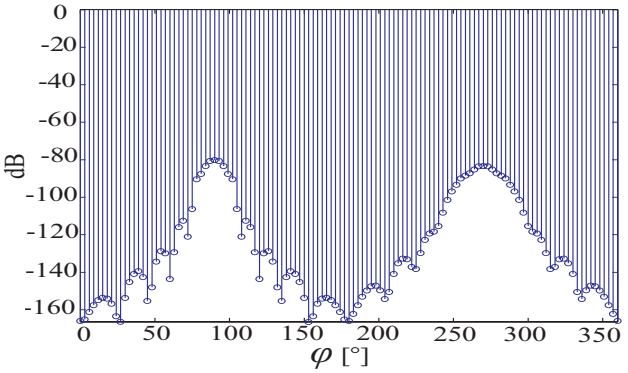

Fig. 10. Search for locations with least error penalty: placing scattering centers at locations where there are no echo sources leads to error in the obtained far-field. Plotted is the energy erroneously attributed to a test scattering center at different locations relative to the AUT total energy.

5 Scattering centers modeling without echo localization

Without knowledge of the echo locations, $\mathbf{C}_{\mathrm{SC}}$, the coupling matrix that describes how an individual echo source contributes to the measured near-field data, cannot be computed. We therefore place the scattering centers around the AUT since, as shown in Fig. 8, such scattering centers can potentially represent components of the echo contributions. In the same way however, these scattering centers can also introduce errors into the obtained far-field pattern as part of the plane waves originating from the AUT might be attributed to the scattering centers during the NFFFT. This scenario is depicted in Fig. 9. To improve the achievable echo suppression without knowledge of the echo locations, we optimize the scattering centers placement by searching for locations where the least amount of error is introduced to the obtained AUT pattern. To this end, an echo free measurement is made and a single scattering center is placed at a particular location during the NFFFT. The NFFFT is repeated several times with the scattering center at varying locations and the attributed energy is recorded. An ideal scattering center location in this scenario will attribute an energy of $-\infty$ dB to the signal originating from the scattering center since the measurement is echo free. The search is done for ϑ fixed at 90° and φ from 0 to 360° with a step of 3°. The result in Fig. 10 shows that the least error is introduced around the null axis of the AUT i.e. along the AUT extended aperture. As a result of this observation, the scattering centers are placed along the plane containing the AUT aperture as shown in Fig. 11 such that no scattering center is placed within the measurement sphere. In this way, the scattering centers replace only the echo sources and components of the AUT signal are not attributed to the scattering centers. The result with this representation is shown in Fig. 12 and the error levels before and after echo suppression in Fig. 13.

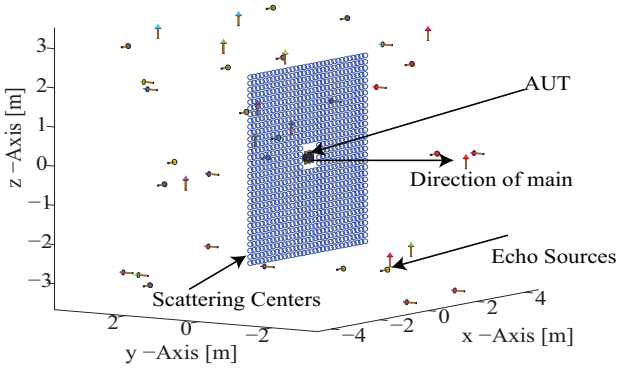

Fig. 11. Scattering centers are placed outside the measurement sphere along AUT extended aperture.

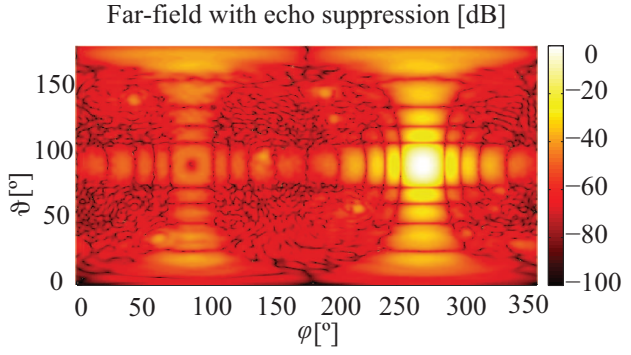

Fig. 12. Far-field after echo suppression without echo localization.

6 Conclusions

We presented methods of modeling echoic measurement environments with auxiliary sources by utilizing the available knowledge about the measurement facility. In situations where the echo locations are known exactly or partially, we simply replace them with scattering centers so that their contributions are integrated within the NFFFT. When the locations are unknown, we optimize the scattering centers placement such that the echo contributions are removed considerably while at the same time keeping the AUT contribution isolated.

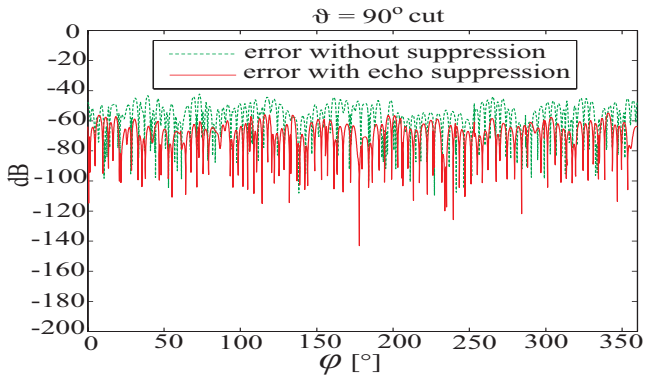

Fig. 13. Error levels before and after echo suppression for the case where the echo locations are unknown.

References

Araque Quijano, J., Vecchi, G., Sabbadini, M., Scialacqua, L., Bencivenga, B., Mioc, F., and Foged, L.: Source reconstruction in advanced processing of antenna measurements, in: Proceedings of the 5th European Conference on Antennas and Propagation (EUCAP), 3875–3879, 2011.

Cano, F., Sierra-Castaner, M., Burgos, S., and Besada, J. L.: Applications of sources reconstruction techniques: Theory and practical results, in: Proceedings of the Fourth European Conference on Antennas and Propagation (EuCAP), 1–5, 2010.

Coifman, R., Rokhlin, V., and Wandzura, S.: The fast multipole method for the wave equation: a pedestrian prescription, IEEE Antenn. Propag. M., 35, 7–12, doi:10.1109/74.250128, 1993.

González, C. G. and Álvarez López, Y.: Characterization of antenna interaction with scatterers by means of equivalent currents, Pr. Electromagn. Res., 116, 185–202, 2011.

Gregson, S., Newell, A., and Hindman, G.: Reflection Suppression in Cylindrical Near-field Antenna Measurememnt Systems, Cylindrical MARS, AMTA 31st Annual Meeting and Symposium, Salt Lake City, 2009.

Hess, D.: Spherical modal filtering of antenna patterns augmented by translation of coordinate origin, in: IEEE International Symposium on Antennas and Propagation (APSURSI), 1632–1635, doi:10.1109/APS.2011.5996615, 2011.

Loredo, S., Pino, M., Las-Heras, F., and Sarkar, T.: Echo Identification and Cancellation Techniques for Antenna Measurement in Non-anechoic Test Sites, IEEE Antenn. Propag. M., 46, 100–107, doi:10.1109/MAP.2004.1296154, 2004.

Saad, Y. and Schultz, M.: GMRES: A generalized minimal residual algorithm for solving nonsymmetric linear systems, SIAM J. Sci. Stat. Comp., 7, 856–869, 1986.

Sarkar, T. and Pereira, O.: Using the Matrix Pencil Method to Estimate the Parameters of a Sum of Complex Exponentials, IEEE Antenn. Propag. M., 37, 48–55, doi:10.1109/74.370583, 1995.

Schmidt, C. and Eibert, T.: Near-field far-field transformation in echoic measurement environments employing scattering center representations, in: 3rd European Conference on Antennas and Propagation, EuCAP 2009, 3370–3374, 2009.

Schmidt, C., Leibfritz, M., and Eibert, T.: Fully Probe-Corrected Near-Field Far-Field Transformation Employing Plane Wave Expansion and Diagonal Translation Operators, IEEE T. Antenn. Propag., 56, 737–746, doi:10.1109/TAP.2008.916975, 2008.

Yaghjian, A.: An overview of near-field antenna measurements, IEEE T. Antenn. Propag., 34, 30–45, doi:10.1109/TAP.1986.1143727, 1986.